Available online at www.sciencedirect.com
SCIENCE DIRECT®
Thermochimica Acta 427 (2005) 207–219
thermochimica acta
www.elsevier.com/locate/tca

Physical organogels: mechanism and kinetics of evaporation of the solvents entrapped within network scaffolding

Nov Markovic, Naba K. Dutta*

Ian Wark Research Institute, ARC Special Research Centre, University of South Australia, Mawson Lakes, SA 5095, Australia

Received 25 March 2003; received in revised form 2 June 2004; accepted 14 September 2004

Abstract

A series of hydrocarbon gels (based on leaded petrol and decalin) using physically crosslinked networks have been prepared using Al-salt of fatty acid as the physical gelling agent. The effects of gel network scaffolding on the mechanism and kinetics of evaporation of the solvents from the gels were investigated using conventional, isothermal and modulated thermogravimetric analysis. It has been clearly observed that the evaporation of solvent from gels followed a complex evaporation pattern compared to the pure solvent. It appears that with increase in network scaffolding the maximum rate of evaporation of the solvent decreases and its distribution become broader. The activation energy of evaporation for these solvents was found not to be dramatically dependent on the concentration of the gelator and tightness of the network scaffolding. Amongst different methods employed, isothermal measurements provided reliable information about the mechanism of evaporation. Modulated thermogravimetric analysis proved to be an efficient method to achieve kinetic parameters of evaporation from a single dynamic experiment. Scanning electron microscopy was used to probe for both dry gelator and gel network after evaporation of the solvents for evaluation of their surface morphology.

Keywords: TGA; MTGA; Evaporation; Organogels; Petrol; Decalin; Kinetics; SEM

1. Introduction

The gels are two-phase non-fluid systems formed by dispersion of a micro molecular liquid in a three-dimensional spongy network formed by supramolecular matrix. The matrix molecules may be linked together by strong intermolecular bond/association among the gel structural elements (forces of physical nature) or may form chemical bond as a result of crosslinking. Irrespective of the nature of the crosslinks formed, gel differs from solution in that it possesses no fluidity, as the local bonds among the matrix molecules form a supramolecular three-dimensional network structure, which does not allow them to move relative to one another [1]. The physical aggregation mechanism may involve a variety of interactions such as: H-bonding, organometallic coordination bonding, Van der Waals forces, electron transfer between donor and acceptor moieties of the gelator, etc. [2]. Because of the transient and reversible nature of the associations, the physical gels exhibit self-healing capacity, and sensitivity to external stimuli (pH, salt, temperature, shear, etc.) that can modulate the self-association propensity, and modify the strength of the connections. Owing to their unique behavior they are receiving significant recent interest as viscosity modifiers in applications such as paints, coatings, oil recovery, control drug release and a variety of pharmaceutical and hygienic applications. The hydrogels (water-based gels), either made from polymers, (biopolymers and synthetic) or by different surfactants are of great importance in every day life and attracted significant research interests. In particular, pharmaceutical applications of a variety of biopolymer gels have been known for centuries [3–5]. However, only a few remarkable investigations have been conducted on non-aqueous (solvent) based gels, on their different syn-

* Corresponding author. Tel.: +61 8 8302 3546; fax: +61 8 8302 3755.
E-mail address: Naba.Dutta@unisa.edu.au (N.K. Dutta).

0040-6031/$ – see front matter © 2004 Elsevier B.V. All rights reserved.
doi:10.1016/j.tca.2004.09.014

thesis methods, characterization techniques and applications [6,7].

The gelation of spilled fuels and/or dangerous solvents hold significant promise in preventing post-spillage disasters by easier cleaning of the affected areas and subsequent recovery of the liquid phase; and have attracted attention since 70s [8–10]. Many investigations on the synthesis of the gelling agents (both physical and chemical types), characterization of the gel network structures, mechanism and kinetics of formation of three-dimensional network, etc., have been published [11–14]. Amongst other physical properties, the thermal behaviour of the gels including the ultimate evaporation of the solvent from the gel network structure is of significant scientific interest and of wide industrial importance. This behavior could also be useful in the understanding of the changes of the gel network structure (scaffolding) of these systems. In this respect hydrogels have been investigated for kinetics of evaporation of water, determination of the different states of water in the gels, degradation of the gels, etc. [15–17]. Important research work also has been carried out on evaporation rates and kinetics from commercial perfumes, explosives, urethane amides, poly(amic acid)s, etc. using TGA [18–21]. Despite some attention and specific studies of the hydrocarbon gel systems for different applications, no detailed investigations on the mechanism and kinetics of evaporation of the solvents from such complex systems have been undertaken [22–24].

In our previous investigations detailed information about the state of the solvent within the physical network structure has been extracted from the DSC investigation of different hydrocarbon gels [22,23]. Rheological investigation has also provided much in-depth information about the gel network structure, morphology, mechanism, kinetics of gel formation and properties [25]. The aim of the current investigation is to evaluate the mechanism and kinetic parameters of solvent evaporation from the gel matrix using conventional and isothermal thermogravimetric analysis (TGA) as well as temperature modulated TGA [26,27]. Two hydrocarbon gel systems has been considered for this investigation: one being very volatile (petrol organogels) and another more stable (decalin organogels). The dried gel networks, after evaporation of all the solvents (xerogels), were examined using scanning electron microscopy (SEM) combined with energy dispersive X-ray analysis (EDX) to achieve morphological information [28,29].

2. Experimental

2.1. Samples

2.1.1. Gel sample preparation

The hydrocarbons used for this investigation were commercially available leaded petrol (gasoline or Super with octane No. 98) and decalin (decahydronaphthalene) from Aldrich, USA. Both the hydrocarbon liquids were used without further purification. The commercial petrol was a mixture of saturated and unsaturated hydrocarbons and could be classified as flammable class IA with flash point <22.8 °C, T_b <37.8 °C and density around 0.72 g ml^{-1}. The solvent decalin was a mixture of *cis*- and *trans*-forms, flash point of 57 °C, T_b of 185–195 °C and density of 0.888 g ml^{-1} [30]. The organogelator used was Calford G-760©, an aluminium salt of fatty acids, procured form Blachford LTEE, Canada and used as received ('ALSP').

The gels were obtained from both hydrocarbons by an in situ method without heating/cooling of the samples. Addition of 'ALSP' powder 'S' (g) into a known volume of solvent (ml) whilst mixing for a specified time (between 1 and 2 min) was performed at ambient temperature (RT). The gels were left for ∼24 h into tightly closed containers to complete formation of equilibrium network. The details of the formulations are presented in Table 1. If the kinetics of gelation is considered qualitatively (at ambient temperature of preparation), different patterns are observed for petrol-based compared to decalin-based organogels. The gelation time for the former range from few seconds to few minutes but for the later it varies from few minutes to few hours depending mostly on the concentration of gelling agent used.

2.1.2. Preparation of xerogels

All petrol organogel samples (Table 1) were exposed to air for seven days for slow drying and minimum disturbance of the surface. After that they were kept under vacuum (1 mm) for additional seven days until completely dry. The surface morphology and elemental analysis of such xerogels were examined using SEM and EDX.

2.2. Thermogravimetric analysis (TGA)

In TGA the mass of a sample is continuously monitored while it is subjected to controlled temperature program in a well-defined atmosphere. All the TGA experiments were carried out using TA Instrument's H-Res/modulated TGA-2950 using dynamic (constant heating rate, d-TGA), isothermal (i-TGA) and modulated temperature thermogravimetric (MTGA) modes. The TGA 2950 instrument is characterized by vertical balance system with sensitivity of 0.1 μg and heating range from room temperature (RT) to 1000 °C. Prior to the experimental runs, temperature calibration of the instrument was performed using the Curie point of Ni [31]. The

Table 1
Formulations of petrol and decalin physical organogels

Gelator ALSP, S (g)	Petrol organogels		Decalin organogels	
	Petrol (wt.%)	Sample label	Decalin (wt.%)	Sample label
0	100	P100	100	D100
1	99	PS1P	99	PS1D
2	97	PS2P	98	PS2D
10	88	PS10P	90	PS10D
20	78	PS20P	82	PS20D
100	0	ALSP100	0	ALSP100

sample weight for all the tests was between 10 and 20 mg, and the samples were placed into an open Al-pan just before inserting into the furnace. The TGA furnace was purged with high-purity N_2 with a flow rate of 50 ml min^{-1}. All the TGA runs were performed in triplicate and the standard error observed to be within 8% in total.

The conventional TGA involved heating the sample from RT, with heating rates of 2, 5, and 15 °C min^{-1}, up to the required final temperature. In isothermal TGA experiments the samples were quickly heated from the ambient to the required temperature and maintaining at the specific temperature until evaporation was completed. For isothermal TGA experiments the temperatures chosen were 50, 60 and 70 °C for petrol, and 70, 80 and 90 °C for decalin gels for different duration of times.

In modulated TGA (MTGA®) an oscillatory temperature program is employed to obtain kinetic parameters in a single experiment. MTGA® was performed with an underlying heating rate of 2 °C min^{-1}, modulation amplitude of ±5 °C min^{-1} and oscillation period of 120 s.

2.3. Scanning electron microscopy (SEM)/energy dispersive X-ray analysis (EDX)

The SEM images on the xerogels were obtained using CamScan Model 44 FE scanning electron microscope operating in an accelerated voltage of 10 kV. The dried samples were sputtered with carbon. The elemental mapping of the experimental samples was performed using EDX [28] to obtain elemental analysis of the sample surface and sub-surface.

3. Results and discussions

3.1. Theory

The kinetics of thermal transformation of a solid-state chemical reaction is generally described for a single step reaction by [32]:

$$r = \frac{d\alpha}{dt} = k(T) f(\alpha) \quad (1)$$

where $f(\alpha)$ is the reaction model, α is the extent of reaction, $k(T)$ is the temperature dependent rate constant, T is the temperature, t is the time, and r is the rate of degradation. The rate constant, $k(T)$ is the normally assumed to obey the Arrhenius equation:

$$k(T) = A \exp\left(\frac{-E}{RT}\right) \quad (2)$$

where E is the activation energy of the kinetic process, A is the pre-exponential factor, and R is the universal gas constant. If it is assumed that the degradation is a simple nth order reaction, the conversion dependent term can be expressed as

$$f(\alpha) = (1-\alpha)^n = W^n \quad (3)$$

where W is the weight-fraction remaining, and n is the order of reaction. Most of the published methods for deriving kinetic parameters from TGA are based upon these three equations.

3.2. Modified single heating run method

Fig. 1 shows the typical plots of the weight loss curves for the experimental decalin organogels, in d-TGA mode with constant dynamic heating rate of 5 °C min^{-1}. After complete solvent evaporation, weight plateau at the level of 'ALSP' present in sample was reached. The differential thermogravimetric (DTG) curves are also presented as inset of the same figure. From the DTG curves indication of the complex evaporation behaviour (at least two component) of the solvent from the network gel structure is clearly evident. It is important to note that from the petrol gels solvent started to evaporate immediately after the start of the run (not presented); however, decalin gels showed some temperature lag (up to 330 K). From the DTG curves the peak temperatures of

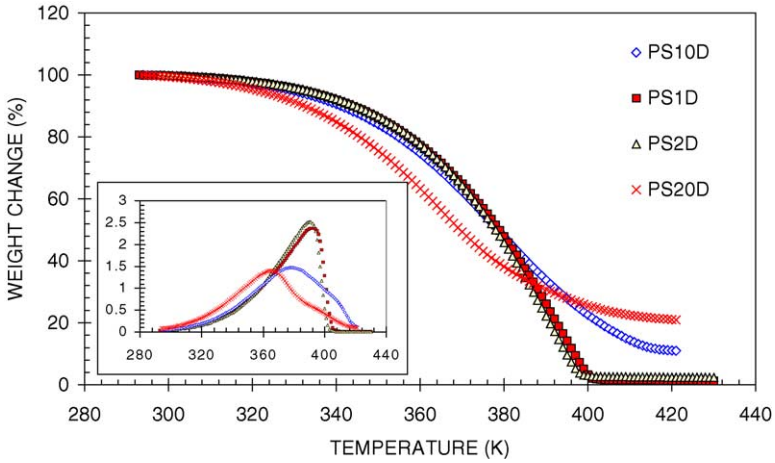

Fig. 1. Weight changes and derivative weight changes (inset) as the function of temperature for decalin organogels (heating rate of 5 °C min^{-1}).

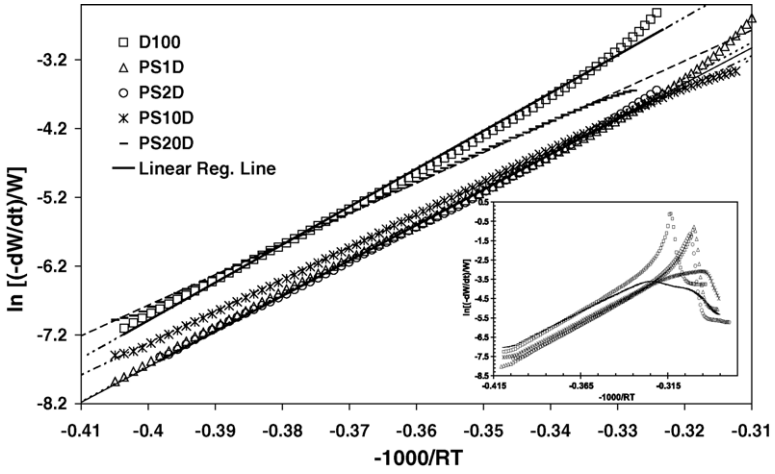

Fig. 2. Linear regression fit of experimental data using Chan-Balke method (decalin organogels) and determination of activation energy E for all ALSP concentrations.

evaporation could be determined as the maximum in derivative weight change. These DTG curves maxima for decalin gels are generally sharper and at higher peak temperatures, if compared to petrol gels (for the same level of 'ALSP'). The gels show strong dependence on concentration of gelator. In general with increase in gelator concentration the distribution of the rate of weight loss curves become wider.

The kinetics of a single step decomposition reactions (including evaporation) in a dynamic heating rate method may be expressed [33,34] as

$$r_{\mathrm{T}} = -\frac{\mathrm{d}W}{\mathrm{d}t} = \frac{A}{\beta}\,\mathrm{e}^{-E/RT}\,W^{n} \tag{4}$$

where r_{T} is the reaction rate, W is the weight fraction of the active material remaining for reaction (g), β is the rate of the heating or thermal ramp (°C min^{-1}). Recently, Chan and Balke [35] proposed a simple method for the evaluation of the kinetic parameters of a reaction from TGA data of a single-constant heating-rate experiment (modification of the method known as Freeman-Carroll [36]). For a first-order reaction, assuming that the order of the reaction remains constant during entire run the equation may be written as [37]:

$$\ln\left(\frac{r}{w}\right) = E\left(-\frac{1}{RT}\right) + \ln A \tag{5}$$

Therefore, for a first-order reaction a plot of $\ln(r/w)$ versus $-1/RT$ should give a straight line with slope equal to the activation energy E. A typical plot of the $\ln[(-\mathrm{d}W/\mathrm{d}t)/W]$ versus inverse temperature ($1000/RT$) for decalin gels (heating rate of 5 °C min^{-1}) is shown as inset of Fig. 2. It appears that the plot deviates from linearity at higher levels of evaporation (above temperature of 385 K); however, it behaves as a first-order process up to ~80% evaporation (see inset of the same figure). In the linear zone of the curves (Fig. 2), linear model fitting (Eq. (5)) was performed to obtain the kinetic parameters of evaporation. The values of E obtained for both petrol and decalin gels are shown in Table 2. Phang [18] examined the activation energy of evaporation of two fixatives (benzophenone and cinnamic acid) and the calculated activation energies at heating rate of 6 °C min^{-1} were observed to be 73 kJ mol^{-1} for benzophenone and 57.4 kJ mol^{-1} for cinnamic acid. The calculated values of the activation energies of evaporation of free solvents at single heating rate of decalin (55 kJ mol^{-1}) and cinnamic acid appear to be close. A marginal but systematic decreasing trend of E, with increase in concentration of gelling agent 'ALSP' is evident. This is to note that the rheological investigations [25] of the gel systems confirmed the dramatic change in the stiffness with marginal change in gelling agent content (particularly in the range of 1.5–5 wt.%). The calorimetric investigation also confirmed significant change in the state of the solvents within the gel network scaffolding with gelling agent content [22,23]. In comparison to those profound changes, however, the change in evaporation rate of the solvent from the network scaffolding and its kinetic parameters with increase gelling agent content are marginal. Therefore, it appears that the diffusion of the solvent molecules under the influence of thermal agitation is not dramatically affected by the network structure formation and its density.

3.3. Multiple heating rates method

Doyle [38] and Flynn and Wall [39] as well independently Ozawa [40] attempted to evaluate E and A as the constants

Table 2
Activation energy E (kJ mol^{-1}) values obtained for pure hydrocarbons (petrol and decalin) as well as their organogels[a]

Petrol gels	P100	PS1P	PS2P	PS10P	PS20P
Chan-Balke method	34	28	27	21	19
Decalin gels	D100	PS1D	PS2D	PS10D	PS20D
Chan-Balke method	55	52	51	46	44

[a] Standard deviation within 5% for petrol-based and within 3% for decalin-based organogels.

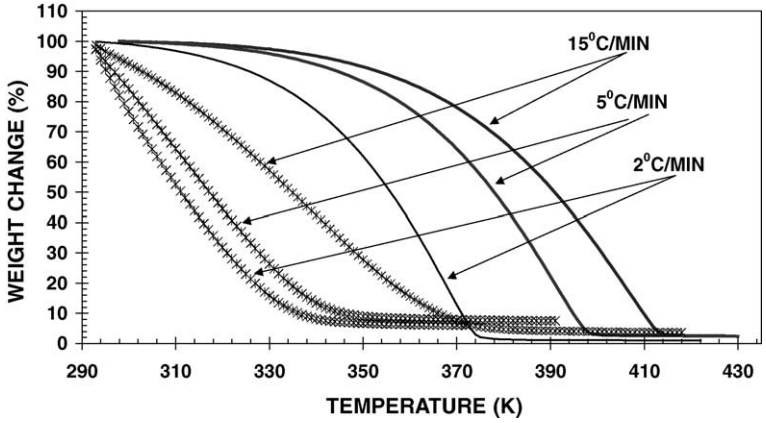

Fig. 3. Effect of different heating rates on the weight change of petrol PS2P (—) and decalin PS2D (★★★★) organogels.

of the equation of the thermogram rather than of the rate equation. They derived a method for the determination of kinetic parameters based on multiple constant heating rates. The final equation developed may be expressed as:

$$\log \beta \cong -0.457\frac{E}{RT} + \left(\log \frac{AE}{RT} - \log F(\alpha) - 2.315\right) \quad (6)$$

If the mechanism of degradation is independent of the heating rate, $F(\alpha)$ is constant for constant α, and the activation energy can be obtained from the slope of the straight-line plot of $\log \beta$ versus '$1/T$' for any level of conversion.

For the calculation of kinetic parameters of evaporation using Eq. (6), TGAs were performed on the experimental hydrocarbon gels using different heating rates (2, 5, and 15 °C min^{-1}) keeping all the other conditions same. Fig. 3 shows typical thermograms for petrol (PS2P) and decalin (PS2D) organogels at different heating rates. From the plots it is evident that the TGA thermogram for a particular gel shifted to higher temperatures systematically as the heating rate increased. It is mainly due to the shorter time required for a sample to reach a given temperature at a faster heating rate. In addition, if decalin gels are compared to the petrol gels, generally, much faster weight changes for the later are observed as expected, due to the higher volatility. All the other experimental gels showed similar trend of weight loss over increased temperature. Applying Eq. (6) and plotting $\log \beta$ versus $1/T$ the slopes of the trend lines through the points, at a specific conversion level would provide activation energy E. The typical plots of $\log \beta$ versus $-1000/RT$ for decalin PS1D (conversion 5–90%) is presented in Fig. 4. In general, a much better straight line fit (the Pearson factor of confidence R^2 almost 99%) was observed for decalin gels. The activation energy calculated for the different experimental gels at different conversion levels are presented in Table 3.

If only conversion levels are considered within the same gel sample in all the cases, E decreases with elapsed reaction time (lowering the solvent quantity available to evaporate from within the network) was evident with no exception. This is a clear indication that the state of the solvent present in all the small cavities within the gel network structure is not in the same state. Initially the relatively free solvent (not held strongly by gel network) evaporated faster followed by tightly

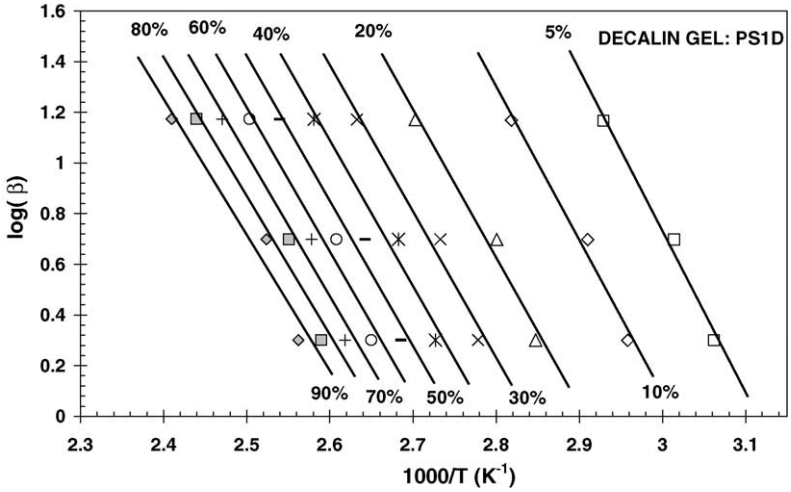

Fig. 4. Dependence of activation energy E on different heating rates (MHR method) at different conversion levels for decalin organogels.

Table 3
Activation energies E (kJ mol^{-1}) obtained by multiple heating rates method for pure solvents petrol and decalin and their physical organogels[a]

Conversion (%)	P100	PS1P	PS2P	PS10P	PS20P
20	81	58	60	68	76
30	77	57	49	53	61
40	65	56	43	46	54
50	56	56	40	42	50
60	48	55	38	40	48
70	42	54	36	38	47
80	40	53	35	36	46
90	39	49	34	34	46
	D100	PS1D	PS2D	PS10D	PS20D
5	81	108	68	53	52
10	65	101	67	45	45
20	56	96	66	41	40
30	52	94	65	38	37
40	51	94	65	36	35
50	49	93	64	34	34
60	48	92	64	32	33
70	47	91	64	30	30
80	46	89	64	29	28
90	46	87	64	28	27

[a] Standard deviation for petrol-based within 4% and for decalin-based organogels within 2%.

entrapped or bound solvent. In general the E values for decalin gels are higher than petrol-based gels. In petrol-based gels gelling agent content has no dramatic effect on E. In the case of comparable decalin gels the activation energy decreased marginally with increase in gelling agent up to PS10P; above that level the value appears to be unaffected.

3.4. Isothermal kinetic study: general rate expression and Flynn methods

For isothermal conditions substituting Eq. (3) into the natural logarithm of Eq. (1), we obtain

$$\ln\left(\frac{-\mathrm{d}W}{\mathrm{d}t}\right) = n\ \ln W + \ln k \tag{7}$$

Therefore, for an nth order degradation, a plot of $\ln(-\mathrm{d}W/\mathrm{d}t)$ against $\ln W$ should result in a straight line with a slope of n, and an intercept on the $\ln(-\mathrm{d}W/\mathrm{d}t)$ axis equal to $\ln k$. The plot of $\ln k$ against $1/T$ then provides activation energy from the slope, and $\ln A$ from the intercept. Eq. (7) is known as the 'General Rate Expression' and used extensively in isothermal thermogravimetric analysis [41]. Fig. 5 illustrates the typical weight loss curves over time for the gels (sample PS1D) at several isothermal temperatures. The rate of evaporation of solvent is also presented in the figure. As expected a faster weight loss and rate of solvent evaporation is observed with increase in the experimental temperature. An indication of the complex nature of evaporation (at least two distinct components) is clearly identified from the derivative weight loss curves. The derivative weight loss curves also reveal that the maximum rate of evaporation occurs not at zero time, but between 2 and 3 min after the isothermal temperature is reached, which indicates that the evaporations are not following simple nth order reaction path. Therefore, complex nature of the evaporation of the entrapped solvents from physical organogels is not following simple nth order reaction path, as previously discussed. Fielden et al. [15] observed that under isothermal conditions microcrystalline cellulose-water gels typically loses 70–80% of the water by a zero order process, indicating that the water is bound to the cellulose rather loosely as free water. However, in the experimental gels the hydrocarbon solvent appears to be present in complex form. Quantitative information about different states of the hydrocarbons in the gels has been analysed by DSC [22,23]. However, from TGA such quantitative information about the different states of the solvent could not be derived.

The plots of $\ln(\mathrm{d}\alpha/\mathrm{d}t)$ against $\ln(1-\alpha)$ for isothermal evaporation (Fig. 6) appear to be not straight over the whole re-

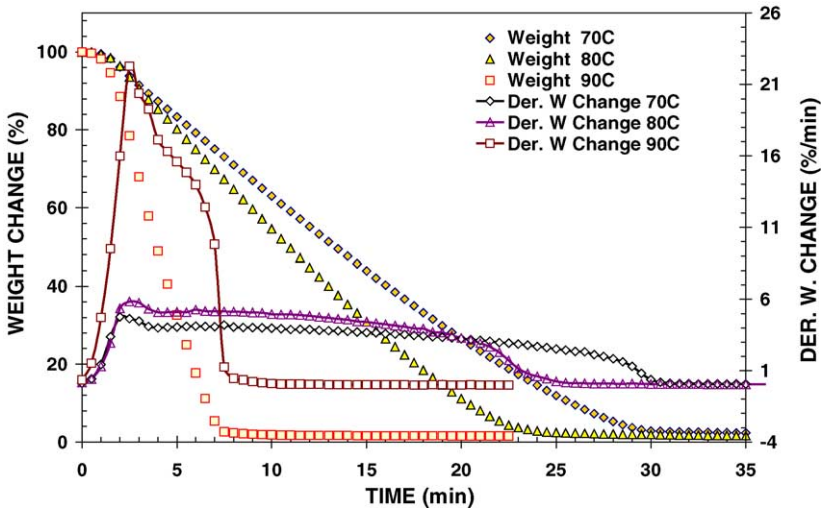

Fig. 5. Change of weight (symbols) and derivative of weight change (symbols with lines) for isothermal TGA (constant temperature) over elapsed time for decalin PS1D.

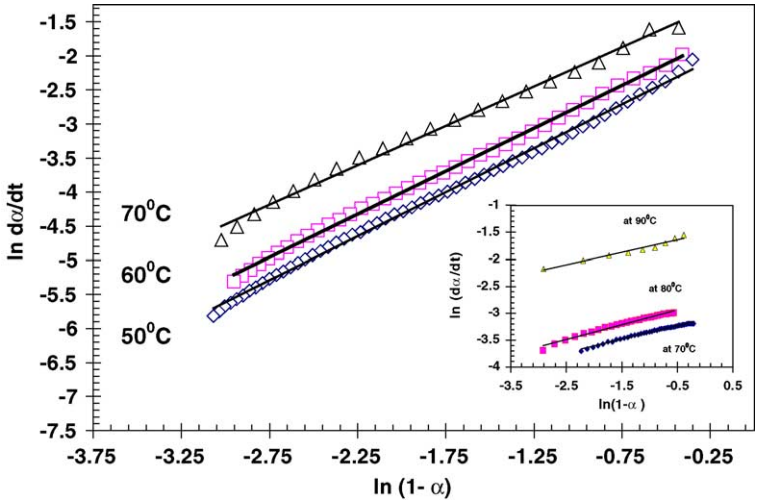

Fig. 6. Calculation of the rate constants K by general rate expression method (isothermal TGA) for petrol PS1P and decalin PS1D (inset) organogels.

gion, however, the region after the peak evaporation in DTGA curve appears to follow a nth order-like exponential decay. This part of the curves can be fitted with a straight line, and can be analyzed using simple nth order method. Such a plot for a typical petrol gel (PS1P) is shown in Fig. 6 (Pearson $R^2 > 94\%$ confidence). Similar plots for the decalin gel (PS1D) are also shown in the inset of the same figure. If the slopes of the lines in similar conditions are compared between the two types of the gels, the less steeper slope of the decalin gels indicate slower evaporation rate of the solvent from the gel networks. The kinetic parameters for different experimental gels calculated using this method are shown in Table 4.

Flynn [42,43] developed a method to calculate the kinetic parameters at different conversion level using isothermal techniques, which may be presented as:

$$\ln t = \ln g(\alpha) - \ln A + \frac{E}{RT} \tag{8}$$

Eq. (8) provides an opportunity to calculate E; if the mode of decomposition remain unchanged during constant test temperature and at α intervals considered, which is based on the slope of a plot of natural logarithm of time against inverse absolute test temperatures, as presented in Fig. 7. The activation energy, E obtained by Flynn method, for different petrol and decalin organogels, are also presented in Table 4. The E values showed some scatters over constant conversion levels if petrol-based gels are compared with decalin-based gels. Again, it is clearly evident that gelling agent concentration has only marginal effect on the kinetic parameters of solvent evaporation from the gel network scaffolding.

3.5. Kinetics of evaporation from the gel networks by MTGA®

Application of sinusoidal temperature program performed by MTGA® produces a change in the rate of weight loss, which provides an experimental tool to study the kinetics of decomposition and volatilization reactions [44,45]

$$E = \frac{[R(T - A^2)L]}{2\mathrm{A}} \tag{9}$$

where A is the temperature amplitude, R is universal gas constant and L is the amplitude of the ln(dα/dt) signal automat-

Table 4
Activation energy E (kJ mol^{-1}) as determined by isothermal TGA methods (general rate expression and Flynn) for petrol and decalin organogels[a]

	Methods for petrol gels			
	P100	PS1P	PS2P	PS10P
Growth rate expression	36	34	42	39
Flynn (at conversion levels (%))				
10	35	37	44	–
20	33	31	35	41
30	30	27	30	37
40	25	23	28	35
50	18	18	22	31
60	14	123	17	25
70	14	6	13	19
80	16	2	63	14
	Methods for decalin gels			
	D100	PS1D	PS2D	PS10D
Growth rate expression	44	38	38	41
Flynn (at conversion levels (%))				
10	62	29	46	46
20	61	31	42	43
30	60	37	37	39
40	58	35	35	36
50	57	37	34	33
60	55	31	33	30
70	52	37	31	27
80	48	37	12	21
90	36	24	22	8

[a] Standard deviation for petrol-based within 5% and for decalin-based organogels within 3%.

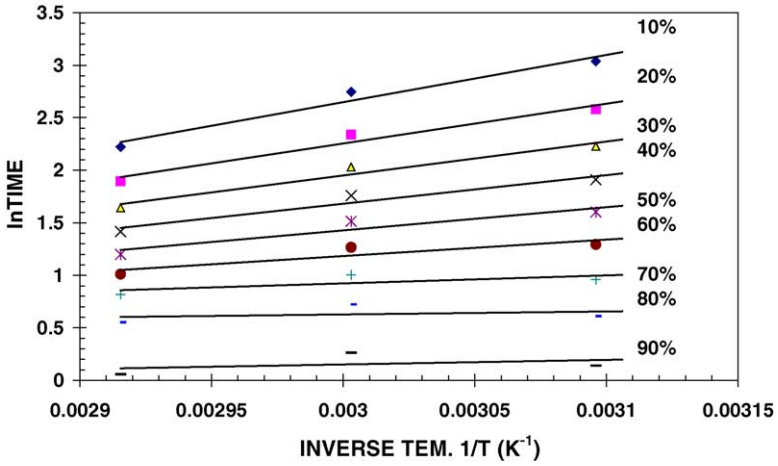

Fig. 7. Flynn method for estimation of activation energy E for decalin organogel PS1D at different levels of conversion (isothermal TGA).

ically obtained by discrete Fourier Transformation. Eq. (9) is considered to be 'model free' equation, because no terms proportional to reaction fraction of constituents are present [46–48]. The typical weight loss and derivative weight loss curves for decalin gels over the range of test temperature are shown in Fig. 8. The weight loss curves appear to be with constant rate up to ∼120 °C, and above that it levels off to quantity of the gelator present in the gels. The weight loss curves shift marginally to higher peak temperatures with gelator concentration up to ALSP content of ∼10 wt.%. Beyond this level DTGA peaks shifts towards lower temperatures with increase in gelator content. Similar results were also observed in petrol-based gels (not shown). In general, the distribution of DTGA curve becomes wider with higher gel content as observed in case of dynamic heating results (Section 3.2).

Fig. 9 shows summary of the activation energy of evaporation E for the petrol-based organogel samples as a function of weight change through evaporation process. For any system considered, a higher level of activation energy is detected at the beginning of the reaction (at weight conversions between 10 and 20%) as well at the end (between 90 and 100%). These changes are expected due to instability of the instrumental parameters. There is a systematic trend in the increase of the absolute values for E with concentration of ALSP in the gels, however the differences in E among the systems are not remarkably high. The neat petrol (P100) showed the highest energy required and could be explained by its very high evaporative nature.

The activation energy of decalin-based organogels also increases marginally but systematically with increase in gelling agent (Fig. 10). Pure solvent (D100) showed the lowest

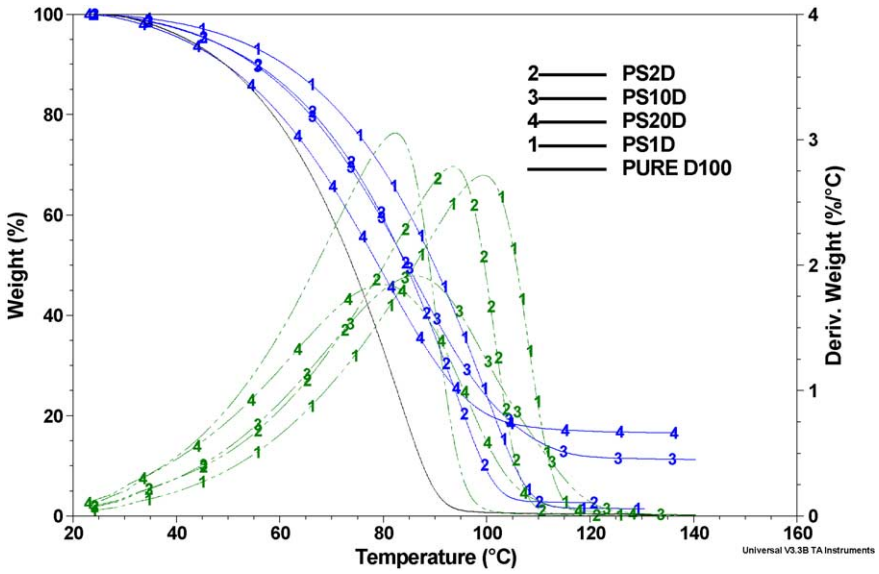

Fig. 8. Changes of the weight and first derivative weight for the decalin-based organogels (different concentrations of ALSP) by MTGA.

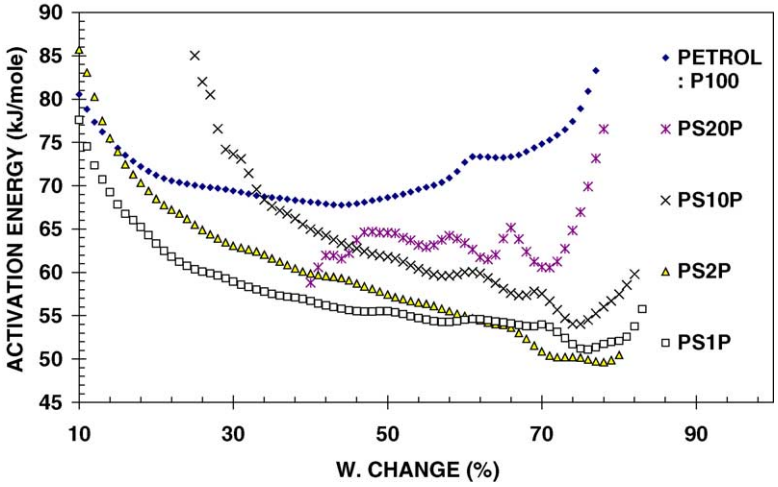

Fig. 9. Estimation of activation energy E as a function of weight change (%) for petrol organogels by MTGA.

activation energy E ~45 kJ mol^{-1}. TGA has been used extensively in the case of hydrogels to enhance the basic understanding of the state of solvent within the gel network scaffolding; as TGA may provide information about the solvent distribution with the system under study. Many investigators also identified various drying regimes, which correspond to different rate controlling steps, and characterized them by differences in drying rates and mechanisms (bound water was more difficult to evaporate than free water) [49]. The presence and quantitative information about the three distinctly different population of solvent (such as free, freezable bound and non-freezable bound solvent) has also been confirmed for the experimental *cis*-decalin-based hydrocarbon gels using DSC [22]. However, from typical TGA/MTGA thermograms the different states of solvents present in the gels systems cannot be identified quantitatively. No individual peak corresponding to the free and lamellar solvent corresponding to the ratio of the different population is evident. There is no significant change in the slope of the weight loss curve observed. Only a qualitative indication of the presence of different state of solvent and its reflection on the complexity of the DTGA curve has been observed. The solvent physical properties, rather than the concentration of the gelling agent were the dominant factors governing evaporation. After Guenet [50] the mechanism of gelation of these physical types of the networks is mainly by solvent induction gelation.

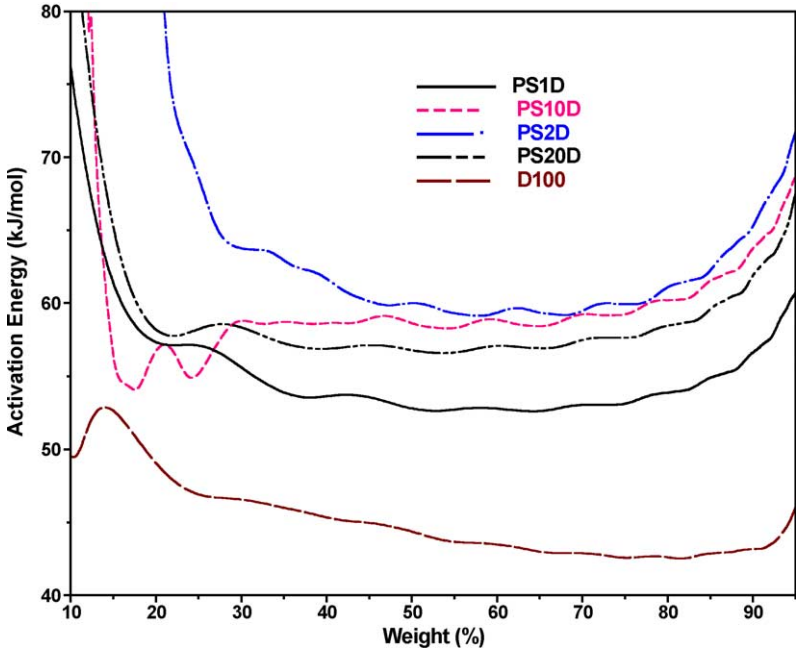

Fig. 10. Estimation of activation energy E as a function of weight conversion (%) for decalin-based organogels by MTGA.

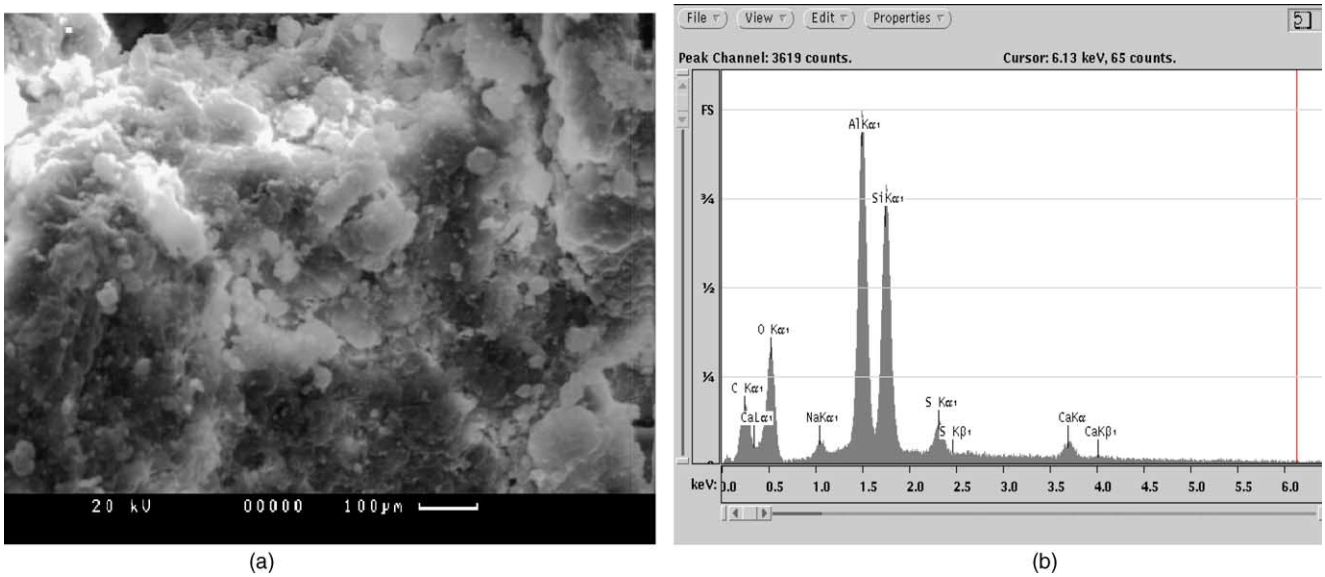

Fig. 11. (a) SEM surface image of pure gelator Calford G-760© and (b) the elemental analysis by EDAX.

At very low level of physical gelling agent the organogel obtained was very soft and very long fiber can be drawn from the gel; with increase in gelator concentration the gel become increasingly firm in consistency. At higher gelator concentration (>5%) the gels are very strong and elastic [25]. At low concentration of gelling agents the self-association among the matrix structure is weak, the network scaffolding is loose and much of the solvent in the gel exists in pools/channels that are sufficiently large such that most of the solvent experience an environment very similar to the pure solvent alone. However, with increase in gelling agent the self-association of the gelling agent creates compact network scaffolding and entraps and isolate tiny amount of solvent within the cellular structure. It is also to note that the solvent used in these experiments is a non-hydrogen bonding type and there is no specific interaction between the solvent and the gelator. These open micro/nano-sponge structures increase the surface area of evaporation significantly and the high nitrogen gas flow rate used has caused rapid forced convection creating a shift in the DTGA profile peak to the lower temperature. Besides that the solvent may be in dynamic equilibrium between different states, and the invasive process of heating the sample may cause changes to the structure, which inevitably alter the temperature range over which the solvent is released. Overall,

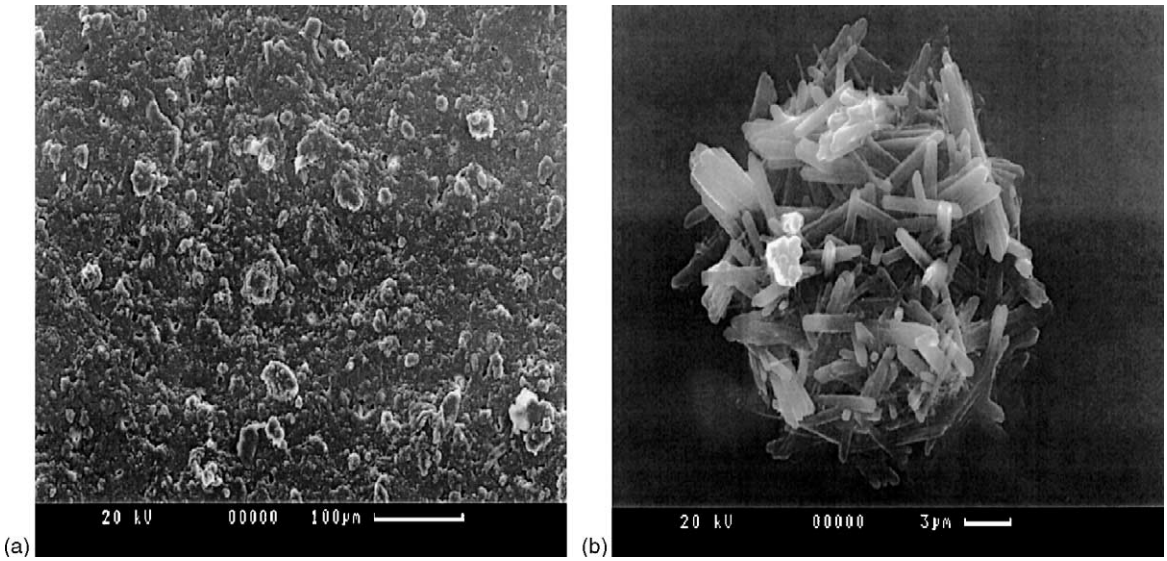

Fig. 12. (a) SEM images of the overall surface of the petrol xerogel, PS2P and (b) enlarged view of the subsurface crystalline fibrils of the gel network scaffolding.

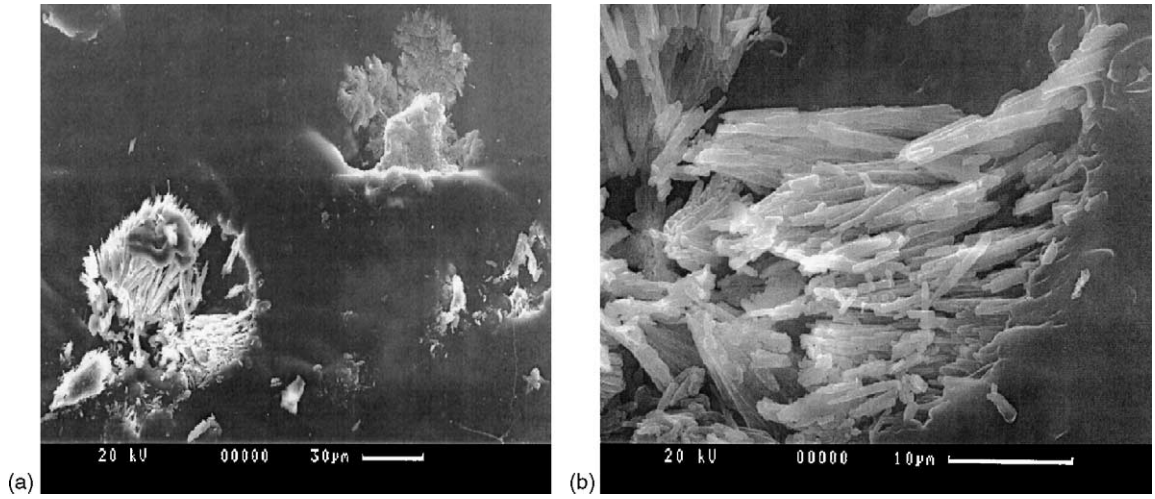

Fig. 13. (a) SEM images of the overall surface of the petrol xerogel, PS4P and (b) enlarged view of the subsurface crystalline fibrils of the gel network scaffolding.

it appears that the molecular diffusion and evaporation of the solvent molecules is not dramatically affected by the tightness of the gel network scaffolding within the experimental range.

3.6. *Effect of the gelator concentration on the morphology of the dried networks of the hydrocarbon organogels*

The appearance of the gel samples surface generally changes after evaporation of the solvent, and imaging of such xerogels may provide insight into the morphology of the gel network scaffolding and therefore mechanism of gelation. Several authors achieved significant in-depth understanding and a diversity of the gel morphologies has been identified using microscopic investigations on the xerogels. Terech and Weiss [7] confirmed the fibrous structures of the steroid and anthryl based organogels using microscopic investigation on the dried gels. Aryl cyclohexanol based xerogels observed to be formed from flexible fibrils [51]. Chan and Mandelkern [52] investigated thermoreversible gelation of low molecular weight linear polyethylene fractions and normal hydrocarbons, and confirmed the formation of the platelike crystallites from polyethylene.

Fig. 11(a and b) shows the surface features of pure physical gelator ALSP (sample ALSP100 in Table 1) and its elemental analysis as detected by SEM and EDX, respectively. From Fig. 11a, the featureless surface of the pure gelator ALSP powder is evident. EDX analysis (Fig. 11b), of the sample indicates that besides Al, O and C (constituent of ALSP), significant amount of elemental Si is also present in the gelator. The presence of Si may be from the dispersant/filler used in ALSP.

Fig. 12a shows the overall surface image for the dried gel network of typical petrol-based sample PS2P. It is evident from the image that after evaporation of the solvent crusty top surface layer was formed. Fig. 12b represents the sub-surface region of the xerogel at higher magnification. Randomly oriented needle-like crystalline fibrils are clearly visible from the image. The diameter and aspect ratio of the fibrils measured to be of 0.6 and 8 μm, respectively. The SEM images of the surface and sub-surface region of xerogel from PS4P are also depicted in Fig. 13a and b, respectively. The images also reveal similar feature as PS2P; however, the crystalline fibrils appear to be more compact in packing and longer in

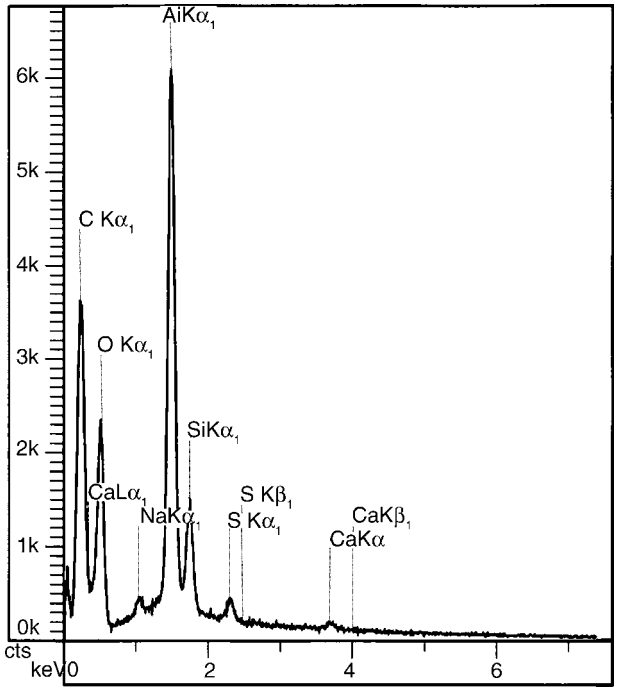

Fig. 14. Elemental composition of the crystalline fibrils as observed by EDAX; (a) xerogel, PS2P, and (b) xerogel, PS4P.

length scale. The average diameter and aspect ratio of the fibrils appear to be 0.65 and 28 μm, respectively. From this observation it may be concluded that gelation is formed due to the three-dimensional network structure formation by the randomly oriented interlocking long thin fibrils, which entrap the solvent and form open nano-sponge structure. The fibrils become longer and the network scaffolding formed by the long needle-like fibrils appears to become tighter with increase in the gelling agent concentration. This observation is in good agreement with Guenet's criterion, that for the thermoreversible gels, the fundamental gel structural element constituted of the fibrils [24].

The elemental analyses on the crystalline fibrils from the gel samples were carried out using EDX and it revealed no significant difference in composition among the different gels (Fig. 14). The ratios between different elements present such as Al to Si (1:0.22), to O (1:0.32) and to C (1:0.52) appear to be similar. The Si peak is remarkably lower in the crystalline fibrils compared to the pure ALSP. This information indicates that the Si containing element does not participate in the crystal formation and thus is not a part of the matrix forming gel network structure. The Si containing substance may act as carrier of the active ingredient, and improve dispersion but do not participate as gelling agent.

4. Conclusions

The mechanism of gelation and kinetic of weight loss for the hydrocarbon gels showed relatively complex behaviour. The interlocking long and thin crystalline fibrils from ALSP appear to form a three-dimensional nano-sponge structure, which entrap solvent to form gel. The compactness of the fibrillar structure and the consistency of the gel network scaffolding increases with increase in the concentration of the gelling agent as observed by SEM. Fibrous structural units of the gel network confirmed physical type of the Al-based organogels.

Although a first-order reaction could explain majority of the changes in activation energy values, its trends obtained appear to be method dependent. Overall, the gelling agent content and the gel network structure does not affect the E value dramatically. Isothermal TGA methods were found to be effective in understanding the mechanism of evaporation. MTGA technique appears to be very effective in obtaining kinetic parameters of evaporation using a single dynamic experiment.

Acknowledgments

The authors would like to thank Prof. J. Matisons for valuable discussions and suggestions. The financial assistance from Defence Science Technology Organization, Australia through joint grant is greatly appreciated.

References

[1] R.F.T. Stepto, in: G. Allen (Ed.), Comprehensive Polymer Science (First Supplement), Pergamon Press, New York, 1992.
[2] P. Terech, in: I.D. Robb (Ed.), Specialist Surfactants, Blackie Academic & Professional, London, 1996.
[3] P.S. Russo, Reversible Polymeric Gels and Related Systems, American Chemical Society, Washington DC, 1987.
[4] T. Tanaka, Scientific American 124 (1981).
[5] Gels in medicine and biology, in: H.B., Bohidar, P. Dubin, Y. Osada (Eds.), Polymer Gels: Fundamentals and Applications, ACS Symposium Series 833, ACS, Washington, 2003, pp. 289–338.
[6] D.J. Abdallah, R.G. Weiss, Langmuir 16 (2000) 352.
[7] P. Terech, R.G. Weiss, Chem. Rev. 97 (1997) 3133.
[8] A. Beerbower, J. Nixon, T.J. Wallace, J. Aircraft 5 (4) (1968) 367.
[9] The Western Company: Gelling Crude Oils to Reduce Marine Pollution from Tanker Oil Spills, for the Water Quality Office Environmental Protection Agency, Project No. 15080 DJN, 1971.
[10] F. Acker, New Scientist (1994).
[11] P.G. De Gennes, Scaling Concept in Polymer Physics, Cornell University Press, New York, 1979.
[12] M. Djabourov, Polym. Int. 25 (1991) 135.
[13] K. Te Nijenhuis, Thermoreversible Networks, Springer-Verlag, Berlin, 1997.
[14] Y. Osada, K. Kajiwara (Eds.), Gels Handbook, vols. 1–4, Academic Press, San Diego, 2001.
[15] K.E. Fielden, J.M. Newton, P. O'Brien, R.C. Rowe, J. Pharm. Pharacol. 40 (1988) 674–678.
[16] A.A. Apostolov, S. Fakirov, E. Vassileva, R.D. Patil, J.E. Mark, J. Appl. Polym. Sci. 71 (1999) 465–470.
[17] M.O. Ngui, S.K. Mallapragada, J. Appl. Polym. Sci. 72 (1999) 1913.
[18] P. Phang, Thermochim. Acta 340/341 (1999) 139.
[19] G.T. Long, S. Vyazovkin, B.A. Brems, C.A. Wight, J. Phys. Chem. B. 104 (2000) 2570.
[20] C.W. Tsimpris, K.G. Mayhan, Thermochim. Acta 3 (1971) 125–132.
[21] S. Bhattacharya, A.S.N. Ghanashyam, Chem. Mater. 11 (1999) 3121–3132.
[22] N. Markovic, M. Ginic-Markovic, N.K. Dutta, Polym. Int. 52 (2003) 1095–1107.
[23] N. Markovic, M. Ginic-Markovic, N.K. Dutta, Benzene physical and chemical organogels: effect of network scaffolding on the thermodynamic behavior of entrapped solvent molecules, J. Appl. Polym. Sci., in press.
[24] J.M. Guenet, Macromol. Symp. 114 (1997) 97–108.
[25] N. Markovic, N.K. Dutta, D.R.G. Williams, J. Matisons, Hydrocarbon gels: rheological investigation of structure, in: H.B. Bohidar, P. Dubin, Y. Osada (Eds.), Polymer Gels: Fundamentals and Applications, ACS Symposium Series 833, ACS Washington, 2003, pp. 190–204.
[26] P.K. Gallagher, Thermogravimetry and thermomagnetometry, in: M.E. Brown (Ed.), Handbook of Thermal Analysis and Calorimetry, Elsevier, Amsterdam, 1998, p. 225.
[27] B. Wunderlich, The basis of thermal analysis, in: E.A. Turi (Ed.), Thermal Characterization of Polymeric Materials, second ed., Academic Press, San Diego, 1997, pp. 205–482.
[28] L.C. Sawyer, D.T. Grubb, Polymer Microscopy, Chapman and Hall, London, 1987.
[29] Y. Lin, B. Kachar, R.G. Weiss, J. Am. Chem. Soc. 111 (1989) 5542–5551.
[30] R.L. Rogers, Directory of Solvents, Blackie Academic & Professional, London, 1996.
[31] R.L. Blaine, in: R. Morgan (Ed.), Proc. 24th N. Am. Therm. Anal. Soc. Conf., McLean, Virginia, 1997.
[32] M.E. Brown, D. Dollimore, A.K. Galwey, Reaction in the Solid State: Comprehensive Chemical Kinetics, Elsevier, Amsterdam, 1980.

[33] P.J. Haines, Thermal Methods of Analysis, Blackie Academic & Professional, London, 1995.
[34] L. Reich, D.W. Levi, Encyclopaedia of Polymer Science and Technology, John Wiley & Sons, New York, 1971.
[35] J.H. Chan, S.T. Balke, Polym. Degrad. Stab. 57 (1997) 135.
[36] E.S. Freeman, B.J. Carroll, J. Phys. Chem. 62 (1958) 394.
[37] C. Gamlin, M.G. Markovic, N.K. Dutta, N.R. Choudhury, J.G. Matisons, J. Therm. Anal. Calor. 59 (2000) 319–336.
[38] C.D. Doyle, J. Appl. Polymer Sci. 5 (1961) 285.
[39] J.H. Flynn, L.A. Wall, J. Natl. Bureau Standards 4 (1966) 323.
[40] T. Ozawa, J. Therm. Anal. 2 (1970) 301.
[41] M. Day, J.D. Cooney, D.M. Wiles, Polym. Eng. Sci. 29 (1) (1989) 19–22.
[42] J.H. Flynn, Thermal Analysis, Academic Press, New York, 1969.
[43] J.H. Flynn, Laboratory Preparations in Macromolecular Chemistry, McGraw-Hill, New York, 1970.
[44] R.L. Blaine, B.K. Hahn, J. Therm. Anal. 54 (1998) 695.
[45] R. Blaine, Am. Lab. (1998) 21–23.
[46] R.R. Keuleers, J.F. Janssens, H.O. Desseyn, Thermochim. Acta 385 (1/2) (2002) 127–142.
[47] C. Gamlin, N. Dutta, N. Roy-Choudhury, D. Kehoe, J. Matisons, Thermochim. Acta 367/368 (2001) 185.
[48] D.M. Price, J. Therm. Anal. Calor. 64 (2001) 315–322.
[49] V.L. Peramal, S. Tamburic, D.Q.M. Craig, Int. J. Pharm. 155 (1997) 91.
[50] J.M. Guenet, Thermoreversible Gelation of Polymers and Biopolymers, Academic Press, London, 1992.
[51] P. Terech, J.J. Allegraud, C.M. Garner, Langmuir 14 (1998) 3991–3998.
[52] E.K.M. Chan, L. Mandelkern, Macromolecules 25 (1992) 5659–5664.